High-spin Isomers in 96Ag: Excitations Across the Z=38 and Z=50, N=50 Closed Shells

Boutachkov, P.; Gorska, M.; Grawe, H.; Blazhev, A.; Braun, N.; Brock, T. S.; Liu, Z.; Singh, B. S. Nara; Wadsworth, R.; Pietri, S.; Domingo-Pardo, C.; Kojouharov, I.; Caceres, L.; Engert, T.; Farinon, F.; Gerl, J.; Goel, N.; Grbosz, J.; Hoischen, Robert; Kurz, N.; Nociforo, C.; Prochazka, A.; Schaffner, H.; Steer, S. J.; Weick, H.; Wollersheim, H. -J.; Faestermann, T.; Podolyak, Zs.; Rudolph, Dirk; Atac, A.; Bettermann, L.; Eppinger, K.; Finke, F.; Geibel, K.; Gottardo, A.; Hinke, C.; Ilie, G.; Iwasaki, H.; Jolie, J.; Kruecken, R.; Merchan, E.; Nyberg, J.; Pfuetzner, M.; Regan, P. H.; Reiter, P.; Rinta-Antila, S.; Scholl, C.; Soderstrom, P. -A.; Warr, N.; Woods, P. J.

Published in:
Physical Review C (Nuclear Physics)

DOI:
10.1103/PhysRevC.84.044311

2011

High-spin isomers in ^{96}Ag: Excitations across the $Z = 38$ and $Z = 50$, $N = 50$ closed shells

P. Boutachkov,[1,*] M. Górska,[1] H. Grawe,[1] A. Blazhev,[2] N. Braun,[2] T. S. Brock,[3] Z. Liu,[4] B. S. Nara Singh,[3] R. Wadsworth,[3] S. Pietri,[1] C. Domingo-Pardo,[1] I. Kojouharov,[1] L. Cáceres,[1] T. Engert,[1] F. Farinon,[1] J. Gerl,[1] N. Goel,[1] J. Grbosz,[5] R. Hoischen,[6] N. Kurz,[1] C. Nociforo,[1] A. Prochazka,[1] H. Schaffner,[1] S. J. Steer,[7] H. Weick,[1] H.-J. Wollersheim,[1] T. Faestermann,[8] Zs. Podolyák,[7] D. Rudolph,[6] A. Ataç,[9] L. Bettermann,[2] K. Eppinger,[8] F. Finke,[2] K. Geibel,[2] A. Gottardo,[4] C. Hinke,[8] G. Ilie,[2] H. Iwasaki,[2] J. Jolie,[2] R. Krücken,[8] E. Merchán,[10] J. Nyberg,[11] M. Pfützner,[12] P. H. Regan,[7] P. Reiter,[2] S. Rinta-Antila,[13] C. Scholl,[2] P.-A. Söderström,[11] N. Warr,[2] P. J. Woods,[4] F. Nowacki,[14] and K. Sieja[14]

[1]*GSi Helmholtzzentrum für Schwerionenforschung, D-64291 Darmstadt, Germany*
[2]*Institut für Kernphysik, Universität zu Köln, D-50937 Köln, Germany*
[3]*Department of Physics, University of York, York YO10 5DD, United Kingdom*
[4]*School of Physics and Astronomy, University of Edinburgh, Edinburgh EH9 3JZ, United Kingdom*
[5]*The Henryk Niewodniczański Institute of Nuclear Physics, PL-31342 Kraków, Poland*
[6]*Department of Physics, Lund University, S-22100 Lund, Sweden*
[7]*Department of Physics, University of Surrey, Guildford GU2 7XH, United Kingdom*
[8]*Physik Department E12, Technische Universität München, D-85748 Garching, Germany*
[9]*Department of Physics, Ankara University, 06100 Tandogan, Ankara, Turkey*
[10]*Departamento de Física, Universidad Nacional de Colombia, Bogotá, Colombia*
[11]*Department of Physics and Astronomy, Uppsala University, S-75120 Uppsala, Sweden*
[12]*Faculty of Physics, University of Warsaw, PL-00681 Warsaw, Poland*
[13]*Department of Physics, Oliver Lodge Laboratory, University of Liverpool, Liverpool L69 7ZE, United Kingdom*
[14]*IPHC, IN2P3-CNRS et Université de Strasbourg, F-67037 Strasbourg, France*

(Received 12 August 2011; published 13 October 2011)

Excited states in ^{96}Ag were populated in fragmentation of an 850-MeV/u ^{124}Xe beam on a 4-g/cm^2 Be target. Three new high-spin isomers were identified and the structure of the populated states was investigated. The level scheme of ^{96}Ag was established, and a spin parity of (13^-), (15^+), and (19^+) was assigned to the new isomeric states. Shell-model calculations were performed in various model spaces, including $\pi\nu(p_{1/2}, g_{9/2}, f_{5/2}, p_{3/2})$ and the large-scale shell-model space $\pi\nu(gds)$, to account for the observed parity changing $M2$ and $E3$ transitions from the (13^-) isomer and the $E2$ and $E4$ transitions from the (19^+) core-excited isomer, respectively. The calculated level schemes and reduced transition strengths are found to be in very good agreement with the experiment.

DOI: 10.1103/PhysRevC.84.044311 PACS number(s): 21.60.Cs, 23.20.Lv, 23.35.+g, 27.60.+j

I. INTRODUCTION

There are many isomeric states predicted and observed near the doubly magic ^{100}Sn nucleus [1,2]. Their existence and properties are governed by the strong proton-neutron ($\pi\nu$) interaction between identical orbitals, and in particular the high-spin $\pi g_{9/2}$ and $\nu g_{9/2}$ orbits. Detailed shell-model calculations provide the tool to probe specific aspects of the nuclear residual interaction through comparison with key experimental data. Of particular interest are cases in the ^{100}Sn region where core-excited high-spin isomeric states may be discovered, as there is a limited number of ways of forming these states. The first and so far only known case of such a state was identified in ^{98}Cd [3]. In fact, this state has a counterpart in the $\mathcal{N} = 3$ harmonic oscillator shell in ^{54}Fe and ^{54}Ni [4]. In the present work we report on the discovery of three isomeric states in the ^{96}Ag nucleus, one of which is a core-excited isomer.

Experimentally there is little known about ^{96}Ag. The existence of an isomeric state was indicated by Grzywacz *et al.* [5], reporting two γ-ray transitions. In the experiment presented here, the power of the Rare Isotope Spectroscopic Investigation at GSI (RISING) setup [6] was used to perform detailed isomer spectroscopy of ^{96}Ag.

II. EXPERIMENT AND RESULTS

The experiment was part of the "stopped beam campaign" of the RISING project [7]. A ^{124}Xe beam with energy of 850 MeV/u and an intensity of 10^9 particles per second was produced at the GSI accelerator complex. The fragmentation reaction on a 4-g/cm^2 ^{9}Be target was employed to produce the excited ^{96}Ag residues, which were thereupon selected with the FRagment Separator (FRS) [8] using the $B\rho - \Delta E - B\rho$ technique. An event-by-event identification was performed with various detectors positioned at the middle (S2) and final (S4) focal planes of the FRS (see, e.g., Fig. 1 of Ref. [9] for the schematic setup). The nuclear charge Z was measured with two multisampling ionization chamber detectors at S4. The mass-over-charge ratio (A/Q) was determined from the measured time of flight between scintillators positioned at S2 and S4. Corrections for different trajectories through the FRS were performed based on position measurements with pairs of time-projection chambers, mounted at S2 and S4. The measured Z and A/Q were corrected for drifts in electronics

*P.Boutachkov@gsi.de

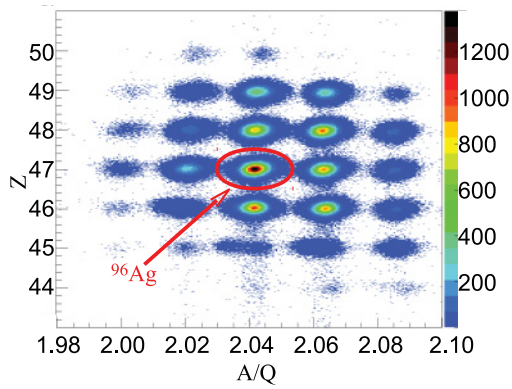

FIG. 1. (Color online) Z versus A/Q identification plot (see text for details).

and temperature and atmospheric-pressure changes during the experiment.

The fragments, including ^{96}Ag, were slowed down with an Al degrader and implanted into an array of nine double-sided silicon strip detectors (DSSSDs), 5×5 cm^2 each, with 16×16 x-y segmentation. The detectors were arranged in three rows with three detectors in each row. The DSSSDs were surrounded by the RISING HPGe detector array, with a layout described in Ref. [7]. The absolute efficiency of the Ge array in this configuration was 10% at 1.3 MeV. DGF-4C [10] modules were used to process the signals from the Ge array within 90 μs after the arrival of an ion at S4. The shortest observed half-lives were limited by the flight time through the separator, about 0.33 μs, and by the background from the prompt bremsstrahlung radiation arising from the implantation of the reaction products in the DSSSDs.

The fragment identification plot obtained in this measurement is shown in Fig. 1 with 2×10^5 ^{96}Ag nuclei identified. The correct reconstruction of Z and A/Q was verified by observing the known γ-ray transitions populated in the isomer decays of ^{96}Pd [11] and ^{98}Cd [3].

The delayed ^{96}Ag γ-ray spectrum acquired up to 90 μs after implantation is shown in Fig. 2, where the γ-ray energies

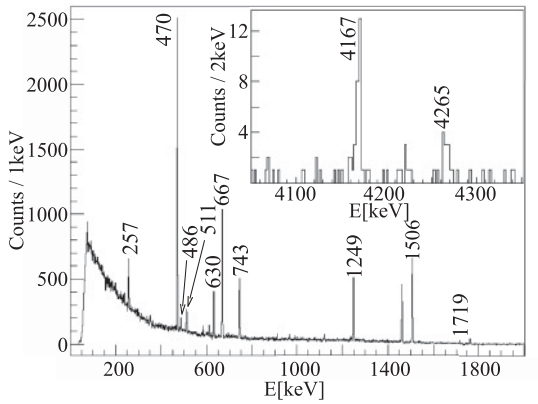

FIG. 2. A γ-ray spectrum observed from 0.075 to 90 μs after implantation of ^{96}Ag. The γ rays associated with ^{96}Ag are marked by their energies. The inset highlights the region around 4 MeV acquired in 0.075 to 0.6 μs after implantation.

of the ^{96}Ag transitions are marked. All γ-ray transitions were observed for the first time in this measurement, except for the 470-keV and 668-keV lines seen by Grzywacz *et al.* [5]. The inset highlights the region around 4 MeV acquired in 0.6 μs after the implantation.

A γ-γ coincidence analysis of the ^{96}Ag data resulted in the level scheme shown in Fig. 3. The isomeric states identified in this experiment are drawn in bold. The level energies, γ-ray energies, E_γ, relative intensities, I_γ, coincidence relations, isomeric ratios [12], R, and the half-lives, $T_{1/2}$, of the measured time distributions are summarized in Tables I and II, respectively. The half-lives for the $2643 + x$-keV and 2461-keV levels were obtained by maximum likelihood fit of the sum of the time distributions for the 470-, 1506-, 1249-, 743-, 257-, 1719-, and 486-keV γ rays (where "x" is the energy of the unobserved transition; see below) with two exponential decay curves. They are consistent with the time distributions of the 630-, 667-, and 743-keV transitions. The half-life of the $6908 + x$ level was obtained by a fit of the sum of the time distributions for the 4167-keV and 4265-keV γ rays with a single exponential decay curve. The summed time distributions are shown in Figs. 4(a) and 4(b), together with the fits. The ordering of the 470-, 1719-, 1976-, and 2461-keV levels is fixed by the cross-over transitions. A γ-ray spectrum in coincidence with the 667-keV transition and a coincidence time window of $\Delta T_c = 0.15$ μs is shown in Fig. 5(a). Because of the narrow coincidence window the γ transitions above the

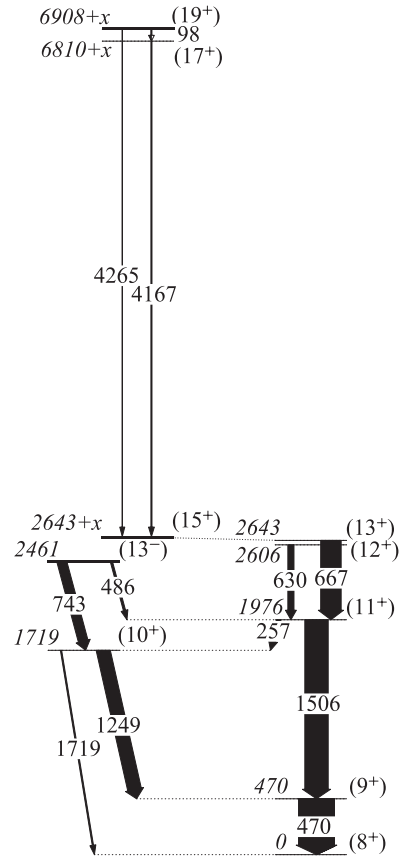

FIG. 3. Proposed level scheme of ^{96}Ag. The isomeric states identified in this experiment are drawn in bold (see text for details).

TABLE I. Level energies, γ-ray energies, relative intensities, and observed prompt coincidences.

E_x (keV)	E_γ (keV)	I_γ	Prompt coincidence transitions(keV)
469.9(2)	470.0(2)	100.0(15)	257,486,630,667,743, 1249,1506
1718.7(2)	1248.8(2)	37.7(12)	257,470,630,667,743
	1718.5(4)	3.4(5)	257,667,743
1975.6(2)	256.8(2)	12.2(8)	470,486,630,667,1249,1719
	1505.7(2)	67.1(15)	470,486,630,667
2461.2(3)	485.7(3)	5.8(6)	257,470,1506
	742.7(2)	26.6(9)	470,1249,1719
2605.7(3)	630.1(2)	18.0(8)	257,470,1249,1506
2643.0(3)	667.4(2)	60.4(12)	257,470,1249,1506,1719
6810(2) + x	4167(2)	2.9(5)	98
6908(2) + x	98(3)		4167
	4265(2)	0.7(3)	

1.56 μs isomer are not visible in this spectrum. In Fig. 5(b) a part of the coincidence spectrum is shown, when ΔT_c is increased to 3 μs and one of the γ rays was detected within 0.6 μs of implantation. The 4167-keV and 4265-keV transitions are marked. This indicates the presence of an isomeric state, with a half-life given in Fig. 4(b), which decays into the state at 2643 + x keV.

A coincidence spectrum of the 1249-keV transition with $\Delta T_c = 0.15$ μs is shown in Fig. 5(c). The 743-keV transition depopulating the 2461-keV level is clearly visible. The 486-keV γ ray is not seen, due to the branching ratios and the observational limit of the RISING array. The 486-keV transition is seen in coincidence with the 257-keV transition. Therefore, it is placed in the level scheme shown in Fig. 3.

The existence of three isomers in ^{96}Ag decaying with high γ multiplicity and partially common cascades, indicates population of high-spin yrast states. In the isotones of ^{96}Ag, ^{94}Rh, and ^{92}Tc, low-lying yrast (8^+) states were observed. These are identified as the ground state or as an isomer at low excitation energy [13,14]. The shell-model calculations in this work and in Ref. [15] predict a low-lying 8^+ state in ^{96}Ag, consistent with the systematics of the (8^+) states in ^{94}Rh and ^{92}Tc. Hence, we have assumed that the lowest state populated by the high-spin yrast cascade in Fig. 3 has $I^\pi = (8^+)$.

The spins of the excited states are assigned assuming the observed transitions follow an yrast decay. Based on the coincidence analysis, the 1719-keV transition is parallel to the 470-keV and the 1249-keV transitions. Hence, it is likely that the 1719-keV transition has an $E2$ character while the 470-keV and 1249-keV transitions have a $M1$ character. Similarly, the 1249-keV and 257-keV transitions form a parallel branch to the 1506-keV transition. There is no isomeric state in between, suggesting $E2$, $M1$, and $M1$ character for the 1506, 1249, and 257 keV transitions, respectively. Therefore, the spins of the 470-keV, 1719-keV, and 1976-keV levels are assigned as (9^+), (10^+), and (11^+). The 630-keV and 667-keV transitions are parallel [see missing coincidence in Fig. 5(a)]. They are in prompt coincidence with the discussed γ rays, and have $T_{1/2}$ of 1.52(5) and 1.54(15) μs, respectively. Hence, the 2606-keV and 2643-keV states (see Fig. 3), are fed by the 1.56-μs isomer. The isomer half-life is compatible only with $E2$ multipolarity and a transition energy close to or below the observational limit of 50 keV. Parallel primary decay branches from the isomeric state to the 2606-keV and 2643-keV levels

TABLE II. Half-lives, $T_{1/2}$, of isomeric states in ^{96}Ag, isomeric ratios, R, and reduced transition probabilities, $B(\sigma\lambda)$, of $E2$, $M2$, $E3$, and $E4$ transitions observed in their decay. One Weisskopf unit (W.u.) corresponds, respectively, to 26.11 e^2 fm^4, 34.59 μ_N^2 fm^2, 547.4 e^2 fm^6, and 12 144 e^2 fm^8 for $E2$, $M2$, $E3$, and $E4$ transitions. Electric transitions are calculated with two sets of effective charges for protons/neutrons: (1.5/0.5) e (a) and (1.72/1.44) e (b).

J_i^π	E_x (keV)	$T_{1/2}$ (μs)	R(%)	J_f^π	σL	E_γ (keV)	$B(\sigma\lambda)$ (W.u.)				
							Expt.	GF		FPG		GDS
								(a)	(b)	(a)	(b)	(a)
(19^+)	6908+x	0.16(3)	2.0(12)	(17^+)	$E2$	98	4.7(10)					3.572
				(15^+)	$E4$	4265	0.9(6)					0.697
(15^+)	2643+x	1.56(3)	10.9(6)	(13^+)	$E2$	$x = 50$	2.45(6)	2.989	4.270	2.983	4.259	3.831
						$x = 25$	6.57(16)					
(13^-)	2461	100(10)	9.0(14)	(11^+)	$M2$ [a]	486	$9.6(14) \times 10^{-5}$			3.57×10^{-5}		
					$E3$[a]		0.62(9)			0.527	0.689	
				(10^+)	$E3$	743	0.145(17)			0.0574	0.128	

[a]Alternative assumption.

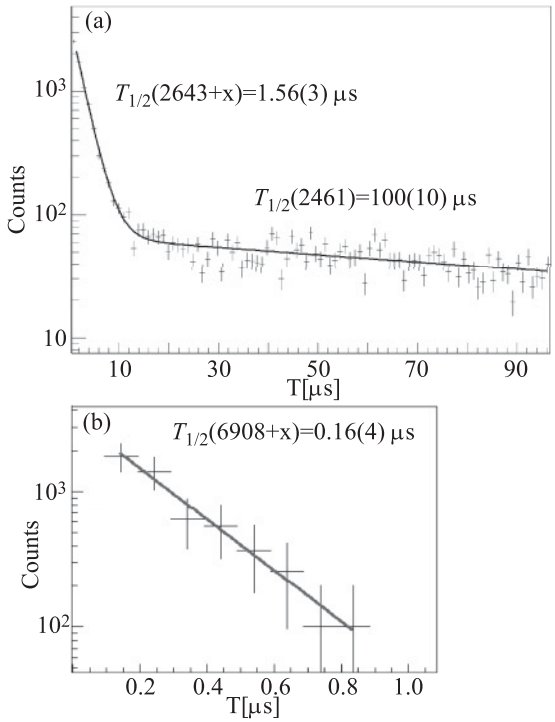

FIG. 4. (a) Summed time distributions for the 470-, 1506-, 1249-, 743-, 257-, 1719-, and 486-keV γ-ray transitions. (b) Sum of the time distributions of the 4167-keV and 4265-keV γ-ray transitions, depopulating the state at 6908 $+ x$ keV. Half-lives are shown, extracted with the maximum likelihood method.

would imply identical spin parity for these states, which is not observed in any of the $N = 49$ odd-odd isotones. Therefore, an $M1$ and $E2$ multipolarity is assigned for the 630-keV and 667-keV transitions, respectively, suggesting a parallel $M1$ cascade of a nondetectable 37-keV transition followed by the

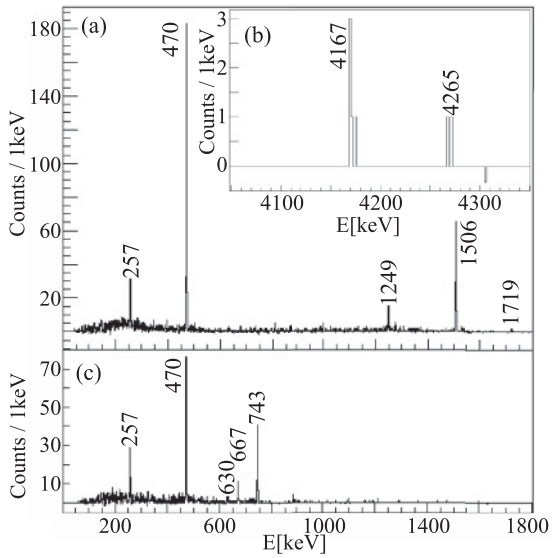

FIG. 5. (a) and (b) Coincidence spectra with the 667-keV transition within time windows of $\Delta T_c = 0.15$ μs and $\Delta T_c = 3$ μs, respectively. (c) A spectrum in coincidence with the 1249-keV transition within a time window of $\Delta T_c = 0.15$ μs.

630-keV transition. This assignment is compatible with the measured intensity ratio. Hence, the tentative spin and parity of the 2606-keV, 2643-keV, and 2643 $+ x$ keV levels [where "x" is the energy of the unobserved $E2$ transition connecting the 1.56-μs isomer to the (13^+) state] are (12^+), (13^+), and (15^+), respectively.

The core-excited 0.16-μs isomer decays by competing 98-keV $E2$ and 4265-keV $E4$ transitions, similar to the core-excited state in ^{98}Cd [16]. This is consistent with the observation of a prompt coincidence between the 98- and 4167-keV transitions. A lower multipolarity for the high-energy transitions is incompatible with the observed half-life and the level scheme. Hence, spins of (17^+) and (19^+) are assigned to the 6810 $+ x$-keV and 6908 $+ x$-keV levels.

The long decay time of the 100-μs isomer and the transition energy indicate a parity changing transition. If the 2461-keV state had a positive parity or the isomer was because of an unobserved low energy $M1$ or $E2$ transition, the 2461-keV state would have been fed from the 2643 $+ x$-keV level. Hence, the data points to a 2461-keV (13^-) state, which decays by 743-keV $E3$ and 486-keV $M2$ transitions. The strength of the $E3$ transition of 0.147(17) W.u. is similar to the $B[E3;(19^-) \rightarrow (16^+)] = 0.3$ W.u. transition strength observed in ^{94}Pd [17].

III. DISCUSSION

The standard shell-model approach to nuclei "southwest" of ^{100}Sn employs empirically fitted interactions in the $(p_{1/2}, g_{9/2})$ proton (π)-neutron (ν) model space (GF) assuming a $^{76}_{38}$Sr$_{38}$ core [18–20]. As this model space does not allow calculation of $M2$ and $E3$ γ-ray transition strengths an extension including the $\pi\nu(p_{3/2}, f_{5/2})$ orbits below $Z = N = 38$ is necessary. Recently the GF space was extended to the $\pi\nu(f_{5/2}, p, g_{9/2})$ space FPG [17] by implementing the GF two-body matrix elements (TBME) [18] with realistic interaction TBME obtained from the CD-Bonn nucleon-nucleon potential [21]. To the latter, core polarization corrections were applied assuming a $^{56}_{28}$Ni$_{28}$ core following the many-body approach of Ref. [22]. Details of tuning to experimental single-particle energies and correction to the GF TBME to avoid double counting of interaction strength are given in Ref. [17]. These approaches, however, cannot account for core excitations across the $N = Z = 50$ shell closure. Therefore, in a third approach the $\pi\nu(g, d, s)$ space GDS with a realistic interaction inferred according to Refs. [21,22] for a $^{80}_{40}$Zr$_{40}$ core was used, as detailed in Refs. [3,16]. However, such a model space cannot describe odd-parity states.

The model spaces and the respective effective interactions employed in the present work in the following are denoted by GF, FPG, and GDS. Shell-model (SM) calculations for GF and FPG were carried out with the code OXBASH [23] while the large-scale shell-model (LSSM) results in the GDS space, allowing for up to $5p$-$5h$ excitations (truncation level $t = 5$), were obtained with the codes ANTOINE and NATHAN [24,25]. Results are shown in Fig. 6 and Table II. Two sets of effective charges were used for electric transitions, namely standard values for large model spaces $e_\pi = 1.5$ e, $e_\nu = 0.5$ e (a) and

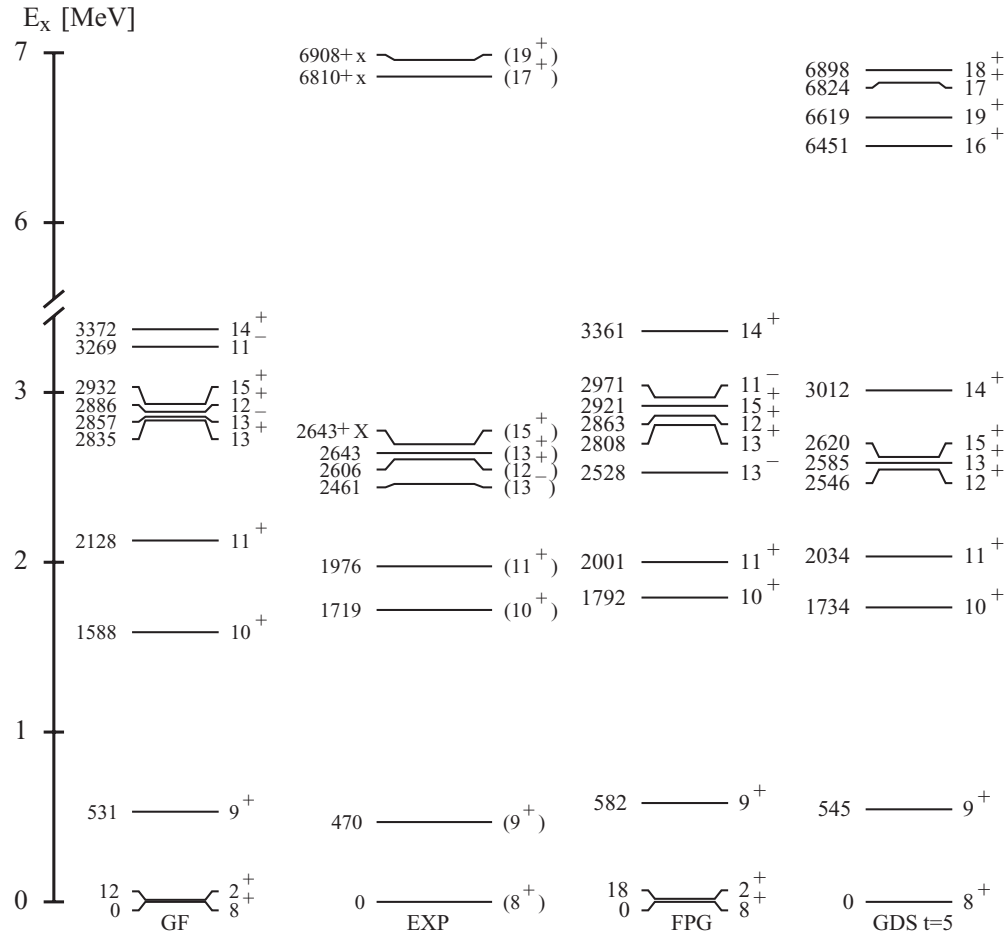

FIG. 6. Experimental and shell-model level schemes for $^{96}_{47}$Ag$_{49}$. See text for details of the shell-model approaches.

$e_\pi = 1.72\ e$, $e_\nu = 1.44\ e$ (b), which was found to be optimum for the small GF model space [20]. For magnetic transitions quenched single-particle g_s factors with $g_s = 0.7\ g_s^{\text{free}}$ were assumed.

The experimental level scheme is very well reproduced by the three approaches within their scope and predictive accuracy. Extension of the GF to the FPG model clearly improves the positions of the 10^+, 11^+, and 13^- levels. The LSSM approach accounts very well for positive parity states and reproduces both the excitation energy and correct order of the $(12\text{-}15)^+$ states including the core-excited isomer. However, it fails in the correct 17^+-19^+ sequence which may be because of details of the interaction. A similar effect was observed in ^{98}Cd for the 12^+-14^+ states [16]. Inspection of the wave functions reveals that the core-excited states in ^{96}Ag are dominated by neutron excitations across the $N = 50$ gap. Therefore, the excitation energy of the isomer is an indirect measure for the ^{100}Sn $N = 50$ neutron gap. The extracted value of 6.70(15) MeV is in fair agreement with the value of 6.46(15) MeV determined for ^{98}Cd [3], which establishes a robust $N = 50$ shell closure for ^{100}Sn. The error in the gap size is an estimate of the systematic uncertainties in the residual interaction.

Electromagnetic transition rates were extracted using the half-lives and intensities listed in Tables I and II and the conversion coefficients of Ref. [26]. The 1.56-μs isomer can be understood as a yrast trap, where a 15^+ state, the highest spin which can be obtained in the $\pi^{-3}\nu^{-1}(g_{9/2}, p_{1/2})$ space, decays by a low-energy $E2$ γ-ray transition. For the experimentally nonobserved $(15^+)\rightarrow(13^+)$ transition two values are given in Table II. The experimental observational limit of 50 keV and the value of 25 keV, below which the total conversion coefficient increases as $\alpha(E2) \sim E_\gamma^{-5}$, which makes the extracted reduced strength independent from the transition energy. Within these experimental limits good agreement with the various shell-model approaches is obtained. The parity-changing transitions, which are forbidden in the GF space, are remarkably well reproduced in the FPG approach if $E3$ multipolarity is adopted for the $(13^-)\rightarrow(11^+)$ transition. In the extended FPG model space the fairly large $E3$ width is because of excitations from the proton $p_{3/2}$ orbit across the $Z = 38$ subshell. The LSSM results in the GDS space using standard effective charges account well for transition strengths between even-parity states including the core-excited (19^+) isomer. The agreement is better than that observed for ^{98}Cd [3]. In contrast to ^{98}Cd, in ^{96}Ag the low-energy $(19^+)\rightarrow(17^+)$ $E2$ dominates over the direct $(19^+)\rightarrow(15^+)$ $E4$ transition owing to the larger $E2$ transition energy and the relative reduced transition strengths.

IV. SUMMARY

In summary, three new high-spin isomers with half-lives of 0.16(3) μs, 1.56(3) μs, and 100(10) μs were discovered in ^{96}Ag. The level scheme of ^{96}Ag was built based on coincidence analysis. The 0.16(3)-μs isomer was identified as the second known core-excited isomer in the ^{100}Sn region. The 100(10)-μs isomer is determined as a decay from a negative-parity state, giving a second data point for an $E3$ transition probability in the region. Shell-model calculations were performed in the model space $\pi\nu(p_{1/2}, g_{9/2}, f_{5/2}, p_{3/2})$, necessary to reproduce the observed $E3$, $M2$ transition probabilities, proving excitations across the $Z = 38$ subshell. A large-scale shell-model calculation within the $\pi\nu(gds)$ model space was performed to study the new data on $Z = N = 50$ core excitation. The general features of ^{96}Ag were reproduced, and the excitation energies and the transition probabilities are well described; furthermore, the robustness of the ^{100}Sn shell gap is confirmed. Fine tuning of the residual particle-hole interaction is needed to reproduce the observed (17^+), (19^+) level sequence.

ACKNOWLEDGMENTS

The authors thank the GSI accelerator staff for the excellent work and M. Hjorth-Jensen for providing the original interaction two-body matrix elements in the FPG and GDS model spaces. This work is supported by the UK STFC, the Swedish Research Council, the German BMBF under Contract Nos. 06KY205I, 06KY9136I, 06MT238, and 06MT9156, and the DFG cluster of excellence Origin and Structure of the Universe.

[1] K. Ogawa, Phys. Rev. C **28**, 958 (1983).
[2] H. Grawe *et al.*, Eur. Phys. J. A **27**, 257 (2006).
[3] A. Blazhev *et al.*, Phys. Rev. C **69**, 064304 (2004).
[4] D. Rudolph *et al.*, Phys. Rev. C **78**, 021301 (2008).
[5] R. Grzywacz *et al.*, Phys. Rev. C **55**, 1126 (1997).
[6] M. Górska *et al.*, Acta Phys. Pol. B **38**, 1219 (2007).
[7] S. Pietri *et al.*, Nucl. Instr. Meth. B **261**, 1079 (2007).
[8] H. Geissel *et al.*, Nucl. Instr. Meth. B **70**, 286 (1992).
[9] A. Garnsworthy *et al.*, Phys. Rev. C **80**, 064303 (2009).
[10] B. Hubbard-Nelson, M. Momayezi, and W. Warburton, Nucl. Instr. Meth. A **422**, 411 (1999).
[11] H. Grawe and H. Haas, Phys. Lett. **120B**, 63 (1983).
[12] M. Pfützner *et al.*, Phys. Rev. C **65**, 064604 (2002).
[13] K. Oxorn, B. Singh, and S. K. Mark, Z. Phys. A **294**, 389 (1980).
[14] C. A. Fields, F. W. N. De Boe, and B. J. Diana, Nucl. Phys. A **401**, 117 (1983).
[15] K. Schmidt *et al.*, Nucl. Phys. A **624**, 185 (1997).
[16] A. Blazhev *et al.*, J. Phys.: Conf. Ser. **205**, 012035 (2010).
[17] T. S. Brock *et al.*, Phys. Rev. C **82**, 061309 (2010).
[18] R. Gross and A. Frenkel, Nucl. Phys. A **267**, 85 (1976).
[19] F. J. D. Serduke, R. D. Lawson, and D. H. Gloeckner, Nucl. Phys. A **256**, 45 (1976).
[20] D. Rudolph, K. P. Lieb, and H. Grawe, Nucl. Phys. A **597**, 298 (1996).
[21] R. Machleidt, Phys. Rev. C **63**, 024001 (2001).
[22] M. Hjorth-Jensen, T. T. S. Kuo, and E. Osnes, Phys. Rep. **261**, 125 (1995); M. Hjorth-Jensen (private communication).
[23] B. A. Brown *et al.*, Oxbash for Windows, MSU-NSCL Report No. 1289 (2004).
[24] E. Caurier and F. Nowacki, Act. Phys. Pol. B **30**, 705 (1999).
[25] E. Caurier *et al.*, Rev. Mod. Phys. **77**, 427 (2005).
[26] T. Kibédi *et al.*, Nucl. Instr. Meth. A **589**, 202 (2008).